Int. J. Nano Dimens., 11 (2): 112-119, Spring 2020

ORIGINAL ARTICLE

Electronic properties of hydrogenated porous Graphene based nanoribbons: A density functional theory study

Roya Majidi[1*], AliReza Karami[2], Khatereh Rahmani[3], Amir Mohammad Khairogli[4]

[1]Department of Physics, Shahid Rajaee Teacher Training University, Lavizan, Tehran, Iran
[2]Department of Chemistry, Shahid Rajaee Teacher Training University, Lavizan, Tehran, Iran
[3]Department of Chemistry, Kabul Polytechnic University, Kabul, Afghanishtan
[4]Departmen of Chemistry, Faryab University, Faryab, Afghanishtan

Received 31 October 2019; revised 03 January 2020; accepted 19 January 2020; available online 28 January 2020

Abstract

The structural and electronic properties of the hydrogenated porous graphene nanoribbons were studied by using density functional theory calculations. The results show that the hydrogenated porous graphene nanoribbons are energetically stable. The effects of ribbon type and ribbon width on the electronic properties of these nanoribbons were investigated. It was found that both armchair and zigzag hydrogenated porous graphene nanoribbons are semiconductors. Their energy band gaps depend on the ribbon width and topological shape of carbon atoms at the edges of the nanoribbons. The band gap of the nanoribbons decreases monotonically with increasing the ribbon width. The semiconducting properties of the hydrogenated porous graphene nanoribbons suggest these ribbons as proper materials for use in future nanoelectronic devices.

Keywords: *Density Functional Theory (DFT); Electronic Properties; Energy Band Gap; Hydrogenated Porous Graphene; Nanoribbon.*

How to cite this article

Majidi R, Karami AR, Rahmani Kh, Khairogli AM. Electronic properties of hydrogenated porous Graphene based nanoribbons: A density functional theory study. Int. J. Nano Dimens., 2020; 11 (2): 112-119.

INTRODUCTION

Carbon has the ability to form a variety of allotropes [1]. Low dimensional carbon allotropes such as fullerene [2], carbon nanotubes [3], graphene and graphyne [4, 5] have attracted a lot of attention due to their special structures and unique properties. In particular, graphene has been extensively studied [6-15]. Graphene is a monolayer of carbon atoms arranged in a honeycomb lattice. The unique properties of graphene, in particular its electronic properties make it an ideal material for use in future nanoelectronic devices. The electronic properties of graphene arise from the existence of Dirac cones, where the valence and conduction bands meet linearly at a single point in the momentum space [6, 16-18]. Hence, graphene is a zero band gap semiconductor named semimetal. The lack of band gap limits the practical applications of graphene in nanoelectronics. To overcome this problem, many methods such as doping, chemical functionalization, and geometrical restrictions have been tried to open and control the energy band gap of graphene [19-32]. For instance, two-dimensional graphene sheet has been manipulated to form quasi one-dimensional strips named graphene nanoribbons [27]. It is shown that the graphene nanoribbons are semiconductors with direct energy band gaps and their energy band gaps are inversely proportional to the ribbon width [27].

Many other two-dimensional carbon networks and their derivatives become objects of interest to optimize the electronic properties of carbon-based nanostructures [25, 29-36]. For instance, hydrogenated porous graphene and biphenylene carbon have been proposed as they have the advantage of retaining some of the graphene properties while being intrinsically nonzero gap

* Corresponding Author Email: *royamajidi@gmail.com*

structures [34, 35]. Furthermore, nanoribbons which use biphenylene as building block were investigated [35, 36]. It was found that the energy band gap of nanoribbons depends on the ribbon width and edge atomic connectivity [35, 36]. In the present work, we have considered nanoribbons based on hydrogenated porous graphene. The structural and electronic properties of these hydrogenated porous graphene nanoribbons were studied using density functional theory (DFT).

COMPUTATIONAL METHOD

All calculations were performed using the OpenMX3.8 package [37] within the framework of DFT. The electron exchange correlation was treated using the Perdew-Burke-Ernzerhof (PBE) formulation of the generalized gradient approximation (GGA) [38]. The basis sets were generated using pseudo atomic orbitals (PAOs). The PAO basis functions were specified by s2p2d1 (two s-state, two p-state, and one d-state radial functions) for C and H atoms, within cutoff radii of basic functions set to the values of 7 Bohr radii. The cutoff energy for the plane wave basis set was taken to be 150 Ry. In the band structure calculations, 21 k-points were considered along Γ (0 0 0) to X (0.5 0 0) direction. The position of all atoms was fully relaxed until the forces on each atom were smaller than, 0.05 eV/Å. The periodic boundary conditions were applied. A vacuum space of 20 Å was considered between two adjacent ribbons to eliminate interaction between the original structure and its periodically repeated images. The charge density difference was also calculated to better understand the nature of bond characteristic.

The cohesive energy, E_{coh}, was calculated to have a measure of the stability of each structure. The cohesive energy represents the energy that would be required to decompose the structure into isolated atoms. It was defined as:

$$E_{coh} = \frac{E_{tot} - (n_C E_C - n_H E_H)}{n_C + n_H} \quad (1)$$

where, E_{tot} , E_C , and E_H are total energy of the ribbon, C and H atoms, respectively. n_C and n_H denote the number of C and H atoms, respectively. Here, negative cohesive energy implies an energetically stable structure.

RESULTS AND DISCUSSION

Before studying the electronic properties of hydrogenated porous graphene nanoribbons, the structural and electronic properties of hydrogenated porous graphene sheet were discussed. The structure of hydrogenated porous graphene sheet can be described as a network of C_6H_3 benzene-like units, interconnected through C-C bonds [31]. The primitive unit cell of hydrogenated porous graphene sheet contains 12 C and 6 H atoms [31, 34]. We have used a supercell with 24 C and 12 H atoms as shown in Fig. 1a to model the infinite hydrogenated porous graphene sheet. Our calculated cohesive energy for hydrogenated porous graphene sheet is -5.87 eV/atom. The negative cohesive energy denotes hydrogenated porous graphene sheet is energetically favorable and can be achieved experimentally. The stability and cohesive energy of hydrogenated porous graphene sheet were reported in previous study [26]. Top view of charge density diagram for hydrogenated porous graphene sheet is illustrated in Fig. 1b. Here, charge density isosurface value of 0.012 e/Å^3 is chosen for the given diagrams. Electron loss and gain are represented by cyan and yellow color isosurfaces, respectively. The results show that electron accumulation is mainly located within the C bonds, while electron depletion occurs around C atoms. It means that the C–C bonds are covalent in nature.

The electronic band structure and density of states (DOS) of hydrogenated porous graphene sheet are shown in Fig. 2. Our results give a band gap of 2.097 eV for hydrogenated porous graphene sheet in good agreement with previous studies [29, 31, 32, 39]. In previous studies, DFT calculations determined the values of 3.2, 2.35, and 2.48 eV, whereas a value of 3.7 eV was measured using the crystal orbital methods [29, 31, 32, 39].

The armchair and zigzag hydrogenated porous graphene nanoribbons were obtained by cutting through an infinite hydrogenated porous graphene sheet along two directions indicated as x and y directions in Fig. 1a, respectively. The nanoribbons were named armchair and zigzag depending on the topological shape of the carbon atoms on the edges. In both cases, we have considered hydrogen termination. Fig. 3 show configurations of the armchair and zigzag hydrogenated porous graphene nanoribbons with widths of 24.61 and 24.16 Å, respectively. The ribbon width, W, is

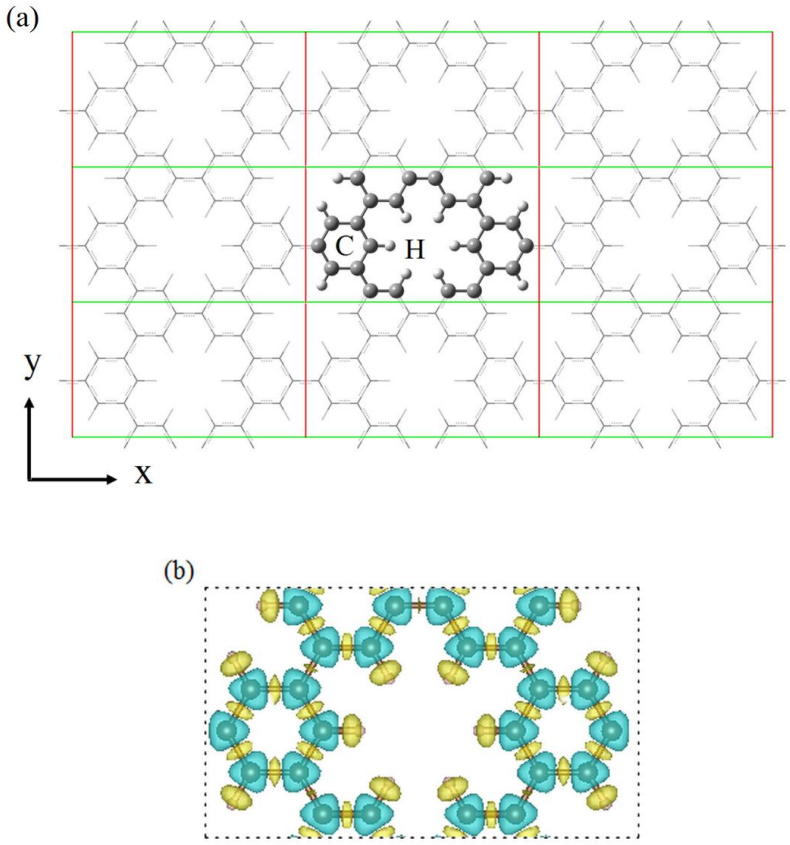

Fig. 1. (a) Atomic structure and (b) top view of charge density difference for hydrogenated porous graphene sheet. (The yellow and cyan regions show the gain and loss of electron, respectively).

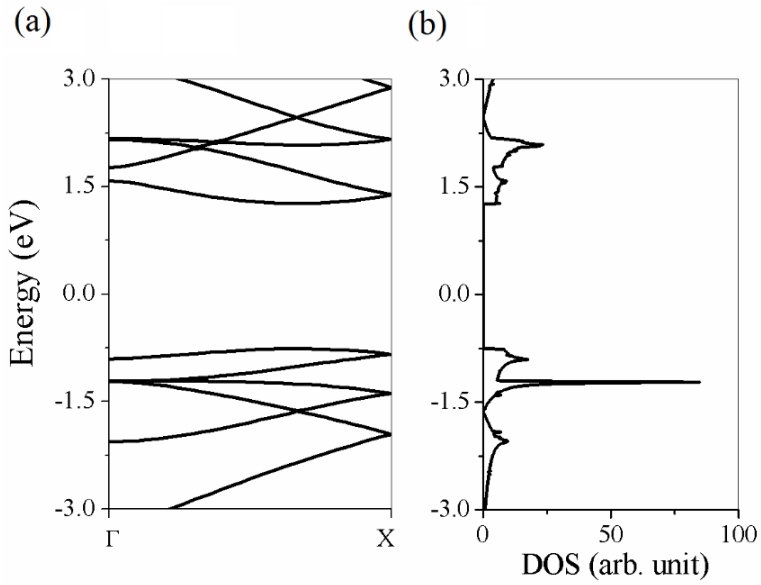

Fig. 2. (a) Electronic band structure and (b) density of states of hydrogenated porous graphene sheet.

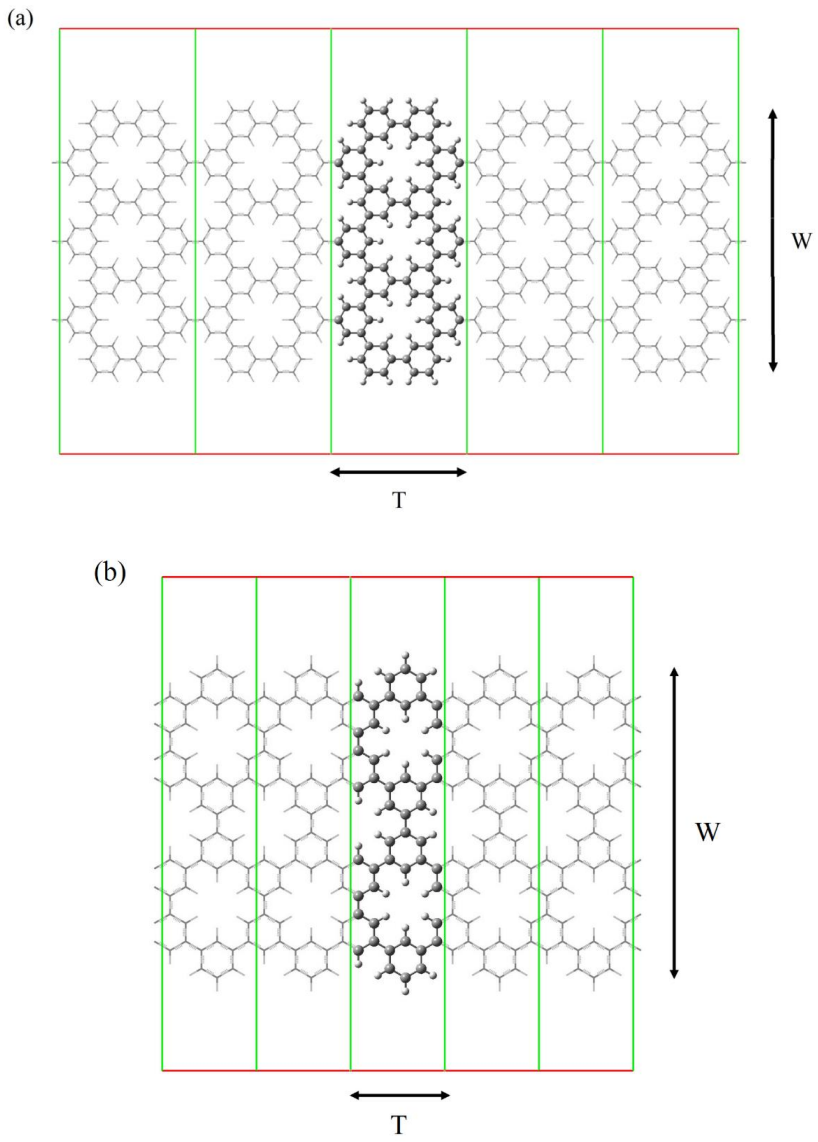

Fig. 3. Atomic structures of (a) armchair nanoribbon with width of 24.61 Å and (b) zigzag nanoribbon with width of 24.16 Å.

measured from the carbon atoms. The unit cell of the armchair and zigzag nanoribbons are marked in Fig. 3, respectively. The lengths of the unit cell, T, are 12.79 and 7.38 Å for the armchair and zigzag nanoribbons, respectively.

As an example, charge density diagrams of the armchair and zigzag hydrogenated porous graphene nanoribbons with widths of 24.61 and 24.16 Å are presented in Fig. 4. Similar to the sheet, electron accumulation and depletion sites are mainly located within the C bonds and around the C atoms, respectively. The C–C bonds are covalent in hydrogenated porous graphene nanoribbons.

The cohesive energies of these nanoribbons as a function of ribbon width are shown in Fig. 5. The negative cohesive energies denote the possibility of experimentally producing hydrogenated porous graphene nanoribbons. Our results also indicate that the cohesive energy of the nanoribbons converges to the cohesive energy of the sheet with increasing the ribbon width (Fig. 5). It means the wide nanoribbons are as stable as the hydrogenated porous graphene sheet.

To study the effect of quantum confinement in the hydrogenated porous graphene sheet, electronic properties of the hydrogenated porous

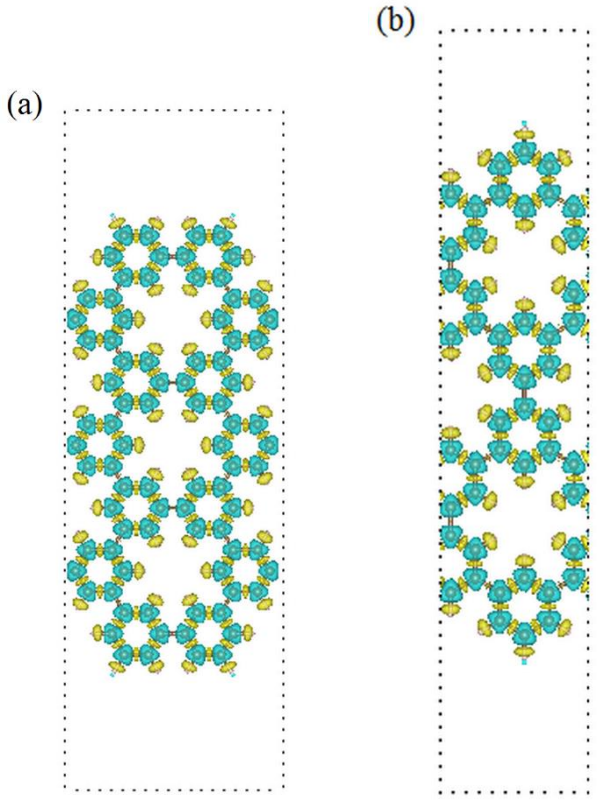

Fig. 4. Top view of charge density difference for (a) armchair nanoribbon with width of 24.61 Å and (b) zigzag nanoribbon with width of 24.16 Å. (The yellow and cyan regions show the gain and loss of electron, respectively).

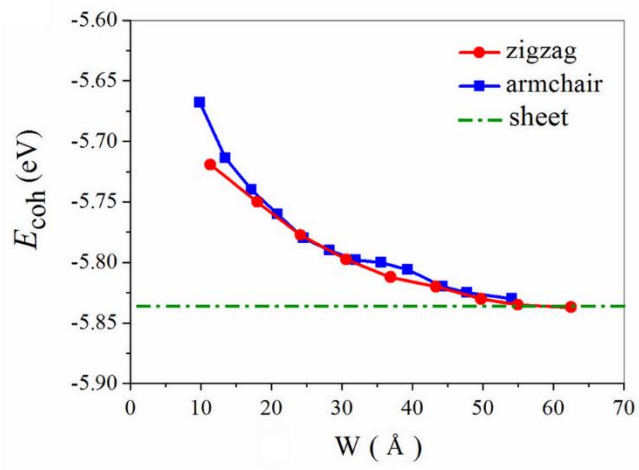

Fig. 5. Cohesive energy of armchair and zigzag nanoribbons as a function of ribbon width.

graphene nanoribbons were studied. For, instance, the electronic band structures and DOS of the armchair and zigzag nanoribbons with widths of 24.61 and 24.16 Å are plotted in Fig. 6 and Fig. 7, respectively. The armchair nanoribbons are found to have a direct band gap between top of the valence band and bottom of the conduction band at the Γ point, and the zigzag nanoribbons have a band gap at a point between the Γ and X point. The DOS is zero at the Fermi level. Hence, these

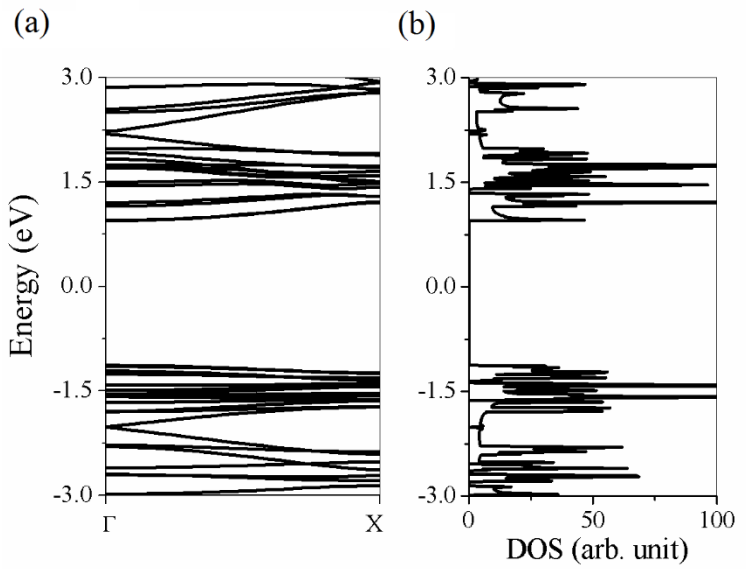

Fig. 6. (a) Electronic band structure and (b) density of states of armchair nanoribbon with width of 24.61 Å.

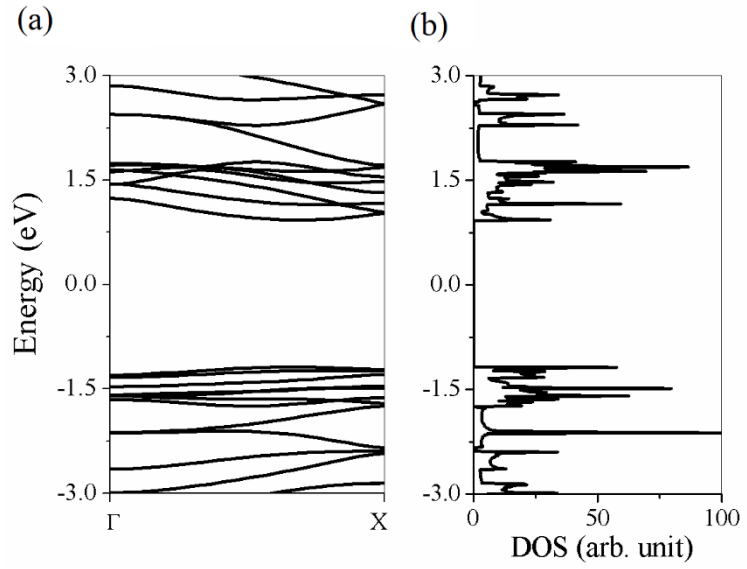

Fig. 7. (a) Electronic band structure and (b) density of states of zigzag nanoribbon with width of 24.16 Å.

nanoribbons have semiconducting properties. The energy band gap of hydrogenated porous graphene nanoribbons as a function of the ribbon width is plotted in Fig. 8. In the present study, the narrowest armchair nanoribbon with width of 9.84 Å and the narrowest zigzag nanoribbon with width of 11.37 Å present band gap of 2.32 eV larger than the band gap of the hydrogenated porous graphene sheet (2.097 eV). Here, the widest considered armchair nanoribbon with width of 54.15 Å and the widest considered zigzag nanoribbon with width of 62.52 Å have band gap of 2.01 eV. It is clear that the band gap decreases monastically as the width of the ribbon increases. The band gap converges to 2.01 eV which is 0.087 eV smaller than the band gap of the hydrogenated porous graphene sheet (2.097 eV). This is because the valence band maximum and the conduction

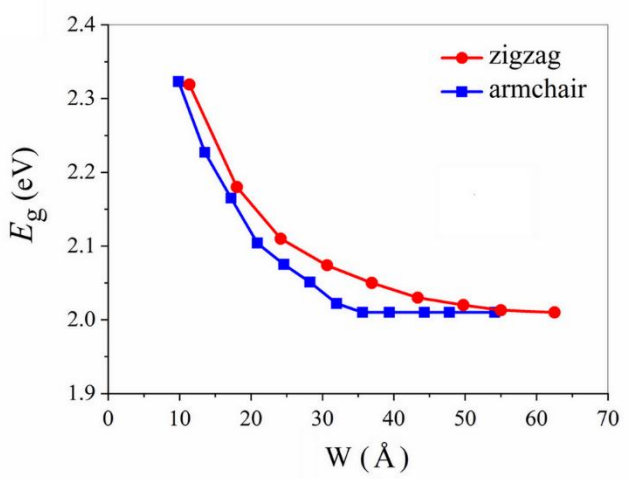

Fig. 8. Energy band gap of armchair and zigzag nanoribbons as a function of ribbon width.

band minimum are determined by edge-states [40]. Our results also indicate that the confinement effects decrease and become negligible with increasing the ribbon width.

CONCLUSION

We have studied the structural and electronic properties of hydrogenated porous graphene nanoribbons using DFT. The cohesive energy, charge density difference, electronic band structure, and DOS were calculated. The negative cohesive energy indicates the considered hydrogenated porous graphene nanoribbons. The C–C bonds of hydrogenated porous graphene sheet and nanoribbons are covalent in nature. The hydrogenated porous graphene nanoribbons with armchair and zigzag type edges were considered. The calculations show that both armchair and zigzag hydrogenated porous graphene nanoribbons present semiconducting properties similar to the hydrogenated porous graphene sheet. The band gap of these nanoribbons decreases monotonically with increasing ribbon width and converges to almost the energy band gap of hydrogenated porous graphene sheet. The rich variety of the electronic properties of hydrogenated porous graphene nanoribbons suggests that these ribbons could be proper materials for use in nanoelectronic devices.

CONFLICT OF INTEREST

The authors declare that they have no competing interests.

REFERENCES

[1] Hofmann R., Hughbanks T., Kertesz M., Bird P. H., (1983), Hypothetical metallic allotrope of carbon. *J. Am. Chem. Soc.* 105: 4831-4832.

[2] Kroto H. W., Heath J. R., OBrien S. C., Curl R. F., Smalley R. E., (1985), C_{60}: Buckminsterfullerene. *Nature*. 318: 162-163.

[3] Iijima S., (1991), Helical microtubules of graphitic carbon. *Nature.* 354: 56-58.

[4] Novoselov K. S., Geim A. K., Morozov S. V., Jiang D., Zhang Y., Dubonos S. V., Grigorieva I. V., Firsov A. A., (2004), Electric field effect in atomically thin carbon films. *Science*. 36: 666-669.

[5] Baughman R. H., Eckhardt H., Kertesz M., (1987), Structure-property predictions for new planar forms of carbon: Layered phases containing sp^2 and *sp* atoms. *J. Chem. Phys.* 87: 6687-6699.

[6] Novoselov K. S., Geim A. K., Morozov S. V., Jiang D., Katsnelson M. I., Grigorieva I. V., Dubonos S. V., Firsov A. A., (2005), Two-dimensional gas of massless Dirac fermions in graphene. *Nature.* 438: 197-200.

[7] Geim A. K., Novoselov K. S., (2007), The rise of graphene. *Nature Mater.* 6: 183-191.

[8] Beitollai H., Safaei M., Tajik S., (2019), Application of graphene and graphene oxide for modification of electrochemical sensors and biosensors: A review. *Int. J. Nano Dimens.* 10: 125-140.

[9] Kivrak H. D., Aktas N., Caglar A., (2019), Electrochemical production of graphene oxide and its application as a novel hydrogen peroxide sensor. *Int. J. Nano Dimens.* 10: 252-259.

[10] Coros M., Pogacean F., Magerusan L., Socaci C., Pruneanu S., (2019), A brief overview on synthesis and applications of graphene and graphene-based nanomaterials. *Front. Mater. Sci.* 13: 23-32.

[11] Mohan V. B., Lau K. T., Hui D., Bhattacharyya D., (2018), Graphene-based materials and their composites: A review on production, applications and product limitations. *Compos. Part B: Eng.* 142: 200-220.

[12] Zhang Q., Wu Z., Li N., Pu Y., Wang B., Zhang T.,

Tao J., (2017), Advanced review of graphene-based nanomaterials in drug delivery systems: Synthesis, modification, toxicity and application. *Mat. Sci. Eng. C.* 77: 1363-1375.

[13] Yang J., Pingan H., Gui Y., (2019), Perspective of graphene-based electronic devices: Graphene synthesis and diverse applications. *APL Mater.* 7: 020901-020905.

[14] Das T., Sharma B. K., Kaiyar A. K., Ahn J-H., (2018), Graphene-based flexible and wearable electronics. *J. Semicond.* 39: 011007-011011.

[15] Yung K. C., Wu W. M., Pierpoint M. P., Kusmartsev F. V., (2013), Introduction to graphene electronics: A new era of digital transistors and devices. *Contemp. Phys.* 54: 233-251.

[16] Geim A. K., (2009), Graphene: Status and prospects. *Science*. 324: 1530-1534.

[17] Castro Neto A. H., Guinea F., Peres N. M. R., Novoselov K. S., Geim A. K. , (2009), The electronic properties of graphene. *Rev. Mod. Phys.* 81: 109-162.

[18] Jalili S., Majidi R., (2006), The effect of gas adsorption on carbon nanotubes properties. *J. Comput. Ther. Nanosci.* 3: 664-669.

[19] Flores M. Z. S., Autreto P. A. S., Legoas S. B. , Galvao D. S., (2009), Graphene to graphane: A theoretical study. *Nanouechnol.* 20: 465704-465709.

[20] Nair R. R., Ren W., Jalil R., Riaz I., Kravets V. G., Britnell L., Blake P., Schedin F., Mayorov A. S., Yuan S., Katsnelson M. I., Cheng H.M. , Strupinski W., Bulusheva L. G., Okotrub A. V., Grigorieva I. V., Grigorenko A. N., Novoselov K. S., Geim A. K., (2010), Fluorographene: A two-dimensional counterpart of teflon. *Small*. 6: 2877-2884.

[21] Majidi R., (2016), Band gap modulation of graphyne via chemical functionalization: A density functional theory study. *Cand. J. Chem.* 94: 229-233.

[22] Majidi R., (2013), Effect of doping on the electronic properties of graphyne. *Nano: Brief Rep. Rev.* 8: 1350060-1350066.

[23] Majidi R., Karami A. R., (2013), Electronic properties of BN-doped bilayer graphene and graphyne in the presence of electric field. *Mol. Phys.* 111: 3194-3199.

[24] Paupitz R., Autreto P. A. S., Legoas S. B., Srinivasan S. G., Van Duin A. C. T., Galvao D. S., (2013), Graphene to fluorographene and fluorographane: A theoretical study. *Nanotechnol*. 24: 035706-035711.

[25] Han M. Y., Ozyilmaz B., Zhang Y., Kim P., (2007), Energy band-gap engineering of graphene nanoribbons. *Phys. Rev. Lett.* 98: 206805-206809.

[26] Perim E., Paupitz R., Autreto P. A. S., Galvao D. S., (2014), Inorganic graphenylene: A porous two-dimensional material with tunable band gap. *J. Phys. Chem. C*. 118: 23670-23674.

[27] Son Y. W., Cohen M. L., Louie S. G., (2006), Energy gaps in graphene nanoribbons. *Phys. Rev. Lett.* 97: 216803-216809.

[28] Lee H., Paeng K., Soo Kim I., (2018), A review of doping modulation in graphene. *Synth. Met.* 244: 36-47.

[29] Ding Y., Wang Y., Shi S., Tang W., (2011), Electronic structures of porous graphene, BN, and BC_2N sheets with one- and two-hydrogen passivations from first principles. *J. Phys. Chem. C*. 115: 5334-5343.

[30] Penhtao X., Jiziang Y., Kesia W., Zhen Z., Panwen S., (2012), Porous graphene: Properties, preparation, and potential applications. *Chinese Sci. Bull.* 57: 2948-2955.

[31] Pierre M. D. L., Karamanis P., Baima J., Orlando R., Pouchan C., Dovesi R., (2013), Ab Initio periodic simulation of the spectroscopic and optical properties of novel porous graphene phases. *J. Phys. Chem. C*. 117: 2222-2229.

[32] Du A., Zhu Z., Smith S. C., (2010), Multifunctional porous graphene for nanoelectronics and hydrogen storage: New properties revealed by first principle calculations. *J. Am. Chem. Soc.* 132: 2876-2877.

[33] Majidi R., Karami A. R., (2017), Nicotine adsorption on BN porous sheets: A density functional theory study. *Rom. Rep. Phys.* 69: 503-508.

[34] Majidi R., Saadat M., Davoudi S., (2017), Electronic properties of o-doped porous graphene and biphenylene carbon: A density functional theory study. *Rom. Rep. Phys.* 69: 509-515.

[35] Denis P. A., (2014), Porous graphitic carbon nitride: A possible metal-free photocatalyst for water splitting. *J. Phys. Chem. C*. 118: 224976-24982.

[36] Hudspeth M. A., Whitman B. W., Barone V., Peralta J. E., (2010), Electronic properties of the biphenylene sheet and Its one-dimensional derivatives. *ACS Nano*. 4: 4565-4570.

[37] Ozaki T., Kino H., Yu J., Han M. J., Ohfuti M., Ishii F., Sawada K., Kubota Y., Mizuta Y. P., Ohwaki T., Ohwaki T., Shiihara Y., Toyoda M., Okuno Y., Perez R., Bell P. P., Ellner M., Xiao Y., Kawamura M., Yoshimi K., Lee C.-C., Terakura K., User's manual of OpenMX version 3.8. http://www.openmx-square.org.

[38] Perdew J. P., Burke K., Wang Y., (1996), Generalized gradient approximation for the exchange-correlation hole of a many-electron system. *Phys. Rev. B*. 54: 16533-16538.

[39] Hatanaka M., (2010), Band structures of porous graphenes. *Chem. Phys. Lett.* 488: 187-192.

[40] Park C. H., Louie S. G., (2008), Energy gaps and stark effect in boron nitride nanoribbons. *Nano Lett.* 8: 2200-2203.